

Magnetic Ordering and Phase Transition in MnO Embedded in a Porous Glass

I. V. Golosovsky,¹ I. Mirebeau,² G. André,² D. A. Kurdyukov,³ Yu. A. Kumzerov,³ and S. B. Vakhruшев³

¹*St. Petersburg Nuclear Physics Institute, 188350, Gatchina, St. Petersburg, Russia*

²*Laboratoire Léon Brillouin, CE-Saclay, F-91191, Gif-sur-Yvette, France*

³*A. F. Ioffe Physico-Technical Institute, 194021, St. Petersburg, Russia*

(Received 9 November 2000)

We present the results of a neutron diffraction study of the antiferromagnet MnO embedded in a porous glass. The type of magnetic ordering and the structural distortion are similar to those of the bulk, but the ordered magnetic moment of $3.84(4)\mu_B/\text{ion}$ is strongly reduced and the Néel temperature is enhanced. The magnetic transition is second order, in contrast to the first order transition of the bulk. The size of the magnetic region is smaller than the average size of the nanoparticles. The reasons for this behavior are discussed.

DOI: 10.1103/PhysRevLett.86.5783

PACS numbers: 75.50.Tt, 61.12.-q, 75.30.Kz

The effects of finite size on the physical properties of condensed matter have attracted great interest. The properties of matter confined to nanometer scale pores or thin films differ from those of the bulk. This has stimulated interest in the behavior of substances in the unusual conditions of so-called “restricted” or “confined” geometry. Moreover, composites consisting of different materials embedded in a porous media have practical applications. For example, it was reported recently that the magnetics sputter deposited onto a nanoporous media are very promising as high-density magnetic storage media [1].

One of the most interesting problems is the influence of a “confined geometry” on a phase transition. In the materials embedded in a porous media, finite-size effects have been studied for melting, freezing [2–4], and superconducting [5] transitions. However, as far as we know, until now there were no experimental data relating to the magnetic phase transitions for materials embedded in a porous media.

In this paper we report the results of a neutron diffraction study of the classic antiferromagnet MnO embedded in a porous glass, where it is present in the condition of a confined geometry. Recent technological progress has made possible the synthesis of different compounds, including magnetic oxides in a glass matrix.

Manganese oxide was selected since the magnetic behavior of the bulk has been well studied. This oxide has an antiferromagnetic structure, for which the magnetic and nuclear Bragg reflections are well separated [6,7]. The magnetic order in bulk MnO occurs by a first order transition at 117 ± 1 K [8], accompanied by a distortion of the cubic structure [7,9].

The porous matrix was made from a sodium borosilicate glass. After a special treatment, an interconnected solid skeleton of nearly pure SiO_2 remains. The matrix has a random interconnected network of elongated pores with a narrow distribution of pore diameters of 70 ± 3 Å. The inner structure of the glass matrix was found to be the same as that reported in [10] (inset in Fig. 1). MnO was synthesized from a manganese nitrate solution by a

chemical bath deposition method, without applying external pressure. The neutron diffraction measurements were performed at the diffractometers G6-1 and G4-1 of the Laboratoire Léon Brillouin with a neutron wavelength of 4.732 Å and 2.427 Å, respectively.

Typical neutron diffraction patterns measured in the paramagnetic and magnetically ordered phases are shown in Fig. 1. New Bragg reflections appearing below 122 K show the onset of correlated magnetic order in the embedded nanoparticles. These diffraction lines are broadened

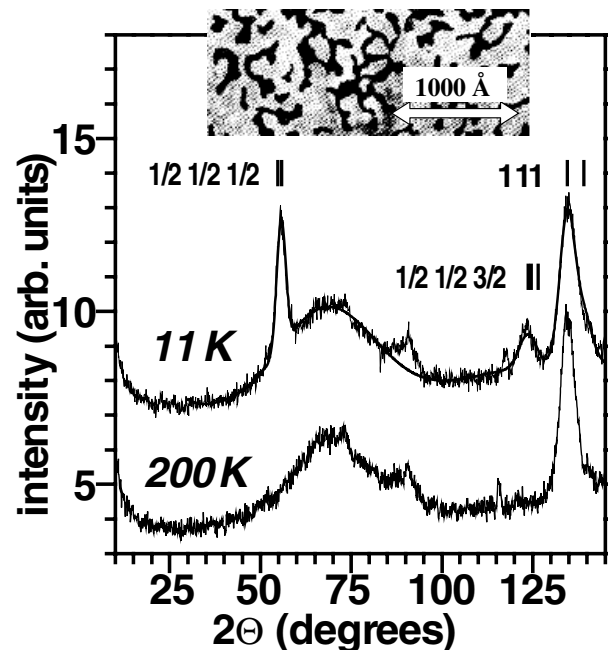


FIG. 1. Neutron diffraction patterns of MnO embedded in a porous glass measured at 11 and 200 K ($\lambda = 4.732$ Å). The stripes mark the positions of Bragg reflections corresponding to the trigonal distorted lattice. Small reflections at about 72° , 90° , and 115° are due to unidentified impurities. The solid line corresponds to the calculated profile. In the top inset the fragment of a typical micrograph of pore network (in dark) from [10] is shown.

with respect to the instrumental resolution, indicating that the correlation length is finite. The observed diffuse background is due to the porous silica glass. The background does not vary with temperature, showing that the sizes of cavities in the glass matrix are temperature independent.

The indexing of the observed magnetic reflections corresponds to antiferromagnetic ordering of type-II in the fcc lattice similar to that reported for bulk MnO [6,7]. The shape of the reflections below the Néel temperature T_N indicates structural distortions and matches to the trigonal distortion of a cubic lattice. The temperature dependencies of the angle of trigonal distortion α and of the unit cell parameter a , shown in Fig. 2, are in good agreement with those reported for bulk MnO [11]. As in the bulk, the anomaly of the unit cell parameter at the magnetic transition, explained by next-nearest-neighbor spin interactions [8,11], is clearly seen in embedded MnO. However, in contrast with bulk, where the angle of trigonal distortions α varies as the square of the mean magnetic moment [11], our data show that in embedded MnO, the angle α is directly proportional to the magnetic moment (Fig. 2b).

From the line-shape analysis of the observed peaks, we calculated the volume-averaged diameters D_{mag} and D_{nucl} for the magnetic and nuclear regions, respectively. Because of the large neutron wavelength, there was a limited number of observed reflections and a strong correlation between the peak width and the crystal distortion parameters. Since the mean diameter of the nanoparticle should be the same below and above the magnetic transition, the width of each of the two components of the nuclear reflection, which is split due to structural distortions below T_N , was kept constant and equal to the peak width above

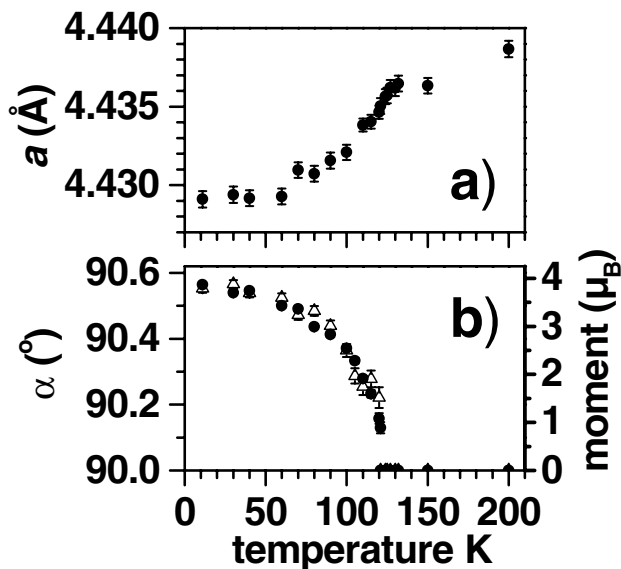


FIG. 2. Temperature dependencies of (a) the unit cell parameter a , and (b) the angle of trigonal distortion α (open triangles) and the magnetic moment (solid circles) for the embedded MnO.

T_N . This value corresponds to the average diameter of the nuclear cluster D_{nucl} of 144(3) Å. The mean diameters of the magnetic regions D_{mag} and nuclear D_{nucl} are shown in Fig. 3. Both values were found significantly larger than the mean pore diameter 70 Å, showing that the confined manganese oxide forms interconnected (probably fractal) aggregates rather than small isolated nanoparticles. Similar aggregates were obtained for gallium particles confined to a porous glass [3,5], where the crystallization spreads at least over several adjacent pores.

The average size of the magnetic cluster turns out to be significantly smaller than the average size of the nanoparticle. The difference between D_{mag} and D_{nucl} could be due to several factors. It could result from a breakdown of the large magnetic aggregates into smaller ones because of necks or other irregularities in a porous media. Since the pore geometry does not change with temperature, such domain formation should only very weakly depend on temperature.

Another explanation could come from the random canting of spins at the surface of the nanoparticle near the pore walls and the formation of a “layer” with spin disorder. As a result, the orientation of the surface magnetic moments could be altered from that in the core. Such disordering is a well-established phenomenon for nanoparticles [12,13]. For example, it was observed in the oxide particles of NiFe_2O_4 [14] and metallic nanoparticles of FeRh [15] and Fe [16].

In metallic particles finite-size effects cause a collective spin freezing at the surface due to a competition between the exchange and anisotropy energies. In oxide nanoparticles surface effects should be more pronounced, since the superexchange magnetic bonds are very sensitive to any nonstoichiometry. The reduced oxygen coordination and the broken bonds at the surface should result in a strong surface disorder.

Recent computer simulations on oxide particles of $\gamma\text{-Fe}_2\text{O}_3$ suggest that magnetic perturbations starting at the surface gradually propagate to the core [17]. However,

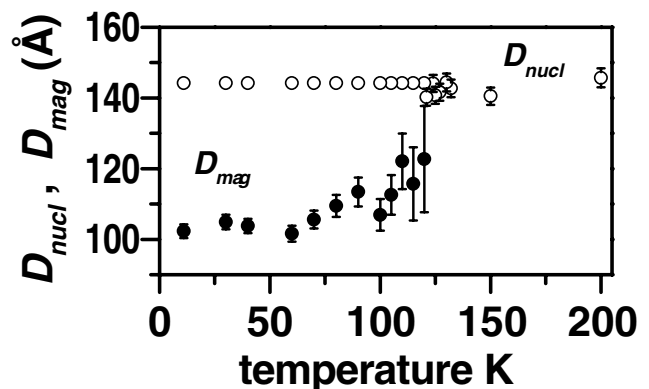


FIG. 3. Temperature dependencies of the volume-averaged diameters D_{mag} (solid circles) and D_{nucl} (open circles) for the magnetic and nuclear regions, respectively, for embedded MnO.

this perturbation becomes smaller with decreasing temperature, in contrast to the present experiment.

In our case the value of D_{mag} should depend on the competition between exchange energy, dominating in core, and some surface energy which arises from the frustration of bonds at the surface, random fields, and others phenomena. This balance could be strongly affected by magnetostriction. The inner stresses due to magnetostriction could result in a change of the exchange interaction distribution at the surface. A quantitative explanation is still lacking.

From the intensity of the magnetic Bragg reflections, the ordered magnetic moment at 10 K was found to be $3.84(4)\mu_B/\text{ion}$. This value, averaged over the magnetic region, turns out to be noticeably smaller than the value of $4.892\mu_B/\text{ion}$ obtained for bulk MnO in the neutron inelastic scattering experiment [18]. In the diffraction experiment the surface spins, disordered on atomic scale, do not contribute to the magnetic Bragg reflections. Therefore, the reduction of the net moment can be explained by random moment canting. Note, that such a moment reduction has been reported for different nanostructured magnetic materials [12].

The temperature dependence of the magnetic moment of the embedded nanoparticles and those in bulk MnO [6] are shown in Fig. 4. It is clearly seen that the discontinuous, first order transition in the bulk becomes continuous in the confined geometry. Fitting the observed magnetic moment dependence $m(T)$ with a power law $m(T) \sim (1 - T/T_N)^\beta$ at $T/T_N > 0.7$ yields the values $T_N = 122.0(2)$ and $\beta = 0.34(2)$. These values should be con-

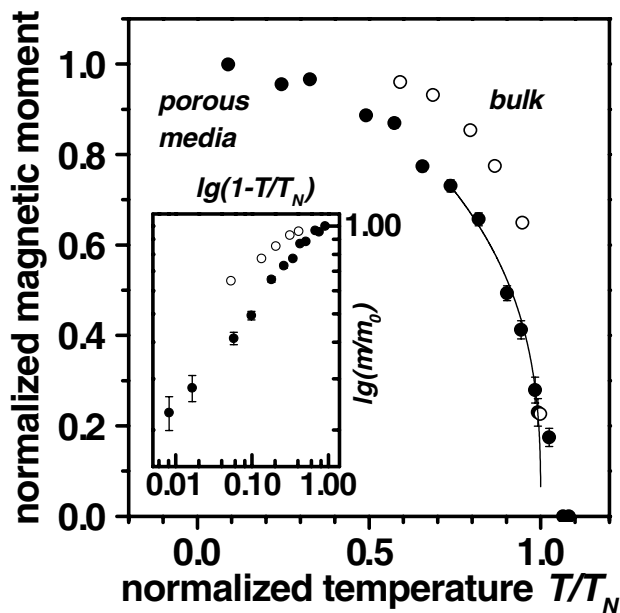


FIG. 4. Temperature dependence of the scaled magnetic moment of MnO embedded in a porous glass (solid circles) and in the bulk MnO (open circles). The solid line corresponds to a fit with a power law. The moment dependencies on a logarithmic scale are shown in the inset.

sidered as low limits because of the quasielastic critical scattering, which exists above the transition. In fact, we see weak traces of quasielastic scattering in the diffraction patterns up to 124 K, that “smears out” a transition. The value of β is close to the critical exponents: 0.362(4) and 0.326(4), obtained by computer simulation of a finite-size scaling for 3D-Ising and 3D-Heisenberg models, respectively [19].

The character of transition depends on several factors: the dimensionality of the space (influence of finite size), the dimensionality of the spin order parameter, and the influence of random fields. The first order transition in bulk MnO was explained quantitatively by using the model of bilinear exchange [8] and by a group-theoretical method with the multicomponent order parameter [20]. The number of components of the order parameter corresponds to the dimensionality of the magnetic irreducible representation.

A second order phase transition, instead of the expected first order, was observed in thin films of MnO [21,22]. The observed change in the character of transition was ascribed to a reduction of the spin order parameter from 8 for the bulk (fourfold symmetry of the wave vector) to 2 for the film (only one magnetic wave vector exists because of strong uniaxial anisotropy). A similar phenomenon was observed in a single crystal MnO under applied pressure [23], when only magnetic domains with one wave vector remain and the transition becomes continuous.

Because of the elongated form of the pores, an anisotropic interaction with the walls of the pores could cause inner stresses and reduce the dimensionality of the spin order parameter. However, in our case MnO was synthesized practically *in situ* inside the pores and it is difficult to expect strong stresses as in films. Therefore, the observed change in the character of transition is unlikely to be due to a change in the dimensionality of the spin order parameter.

Rigorously, singularities at phase transitions occur in the thermodynamical limit only, when the system is infinite along some directions in space [24]. If the system is finite along all dimensions, it cannot exhibit a singular behavior. Computer simulation of phase transition in finite-size systems, in particular, in pores of an aerogel, confirms this general conclusion [25].

In embedded MnO the transition temperature was found to be higher than in the bulk. A general effect of reduced space dimensionality is a strong decrease of T_N . This decrease was observed in a system of ultrafine particles of MnO, randomly distributed on a two-dimensional plane [26]. However, in thin epitaxial films of MnO the transition temperature strongly depends on the substrate and can be either above or below the bulk value [21]. Moreover, there are experimental and theoretical proofs that, even in the same matrix, T_N depends on the size of confined nanoparticles [27]. Probably, this phenomenon depends on the connectivity of adjacent nanoparticles driven

by some specific features of the matrix, such as the wetting of the walls by the embedded material.

In conclusion, by using neutron diffraction the magnetic order in a confined geometry was observed for the antiferromagnet MnO embedded in a porous glass. The type of magnetic order and structural distortion was found to be the same as in the bulk. However, the angle of trigonal distortion is proportional to the magnetic moment, in contrast with the bulk, where this angle is proportional to the square of the magnetic moment. The ordered magnetic moment of $3.84(4)\mu_B/\text{ion}$ is noticeably smaller than in the bulk. The magnetic order extends over a region smaller than the average size of the nanoparticle. Moreover, the magnetic phase transition was found to be second order with an enhanced T_N , in contrast to the first order transition in bulk.

We thank N. Kartenko and N. Sharenkova for x-ray analysis of the samples. This work was supported by the Russian Foundation for Basic Researches (99-02-17273 and 01-02-17739), Russian Federal Foundation for Neutron Studies on Condensed Matter, and Russian Grant "Solid State Nanostructures" (No. 99-1112).

-
- [1] J. Weston, A. Butera, D. Otte, and J. Barnard, *J. Magn. Mater.* **193**, 515 (1999).
- [2] Yu. A. Kumzerov, A. A. Nabereznov, S. B. Vakhrušev, and B. N. Savenko, *Phys. Rev. B* **52**, 4772 (1995).
- [3] E. V. Charnaya, C. Tien, K. J. Lin, and Yu. A. Kumzerov, *Phys. Rev. B* **58**, 11 089 (1998).
- [4] W. Goldburg, F. Aliev, and X-L. Wu, *Physica (Amsterdam)* **213A**, 61 (1995).
- [5] E. V. Charnaya, C. Tien, K. J. Lin, C. S. Wur, and Yu. A. Kumzerov, *Phys. Rev. B* **58**, 467 (1998).
- [6] C. G. Shull, W. A. Strauser, and E. O. Wollan, *Phys. Rev.* **83**, 333 (1951).
- [7] W. L. Roth, *Phys. Rev.* **110**, 1333 (1958).
- [8] M. E. Lines and E. D. Jones, *Phys. Rev.* **139**, A1313 (1965).
- [9] D. Bloch and R. Maury, *Phys. Rev. B* **7**, 4883 (1973).
- [10] P. Levitz, G. Ehret, S. K. Sinha, and J. M. Drake, *J. Chem. Phys.* **95**, 6151 (1991).
- [11] B. Morosin, *Phys. Rev. B* **1**, 236 (1970).
- [12] R. H. Kodama, *J. Magn. Magn. Mater.* **200**, 359 (1999).
- [13] A. E. Berkowitz and K. Takano, *J. Magn. Magn. Mater.* **200**, 552 (1999).
- [14] R. H. Kodama, A. E. Berkowitz, E. J. McNiff, Jr., and S. Foner, *Phys. Rev. Lett.* **77**, 394 (1996).
- [15] A. Hernando, E. Navarro, M. Multigner, A. Yavari, D. Fiorani, M. Rosenberg, G. Filoti, and R. Caciuffo, *Phys. Rev. B* **58**, 5181 (1998).
- [16] E. Bonetti, L. Del Bianco, D. Fiorani, D. Rinaldi, R. Caciuffo, and A. Hernando, *Phys. Rev. Lett.* **83**, 2829 (1999).
- [17] H. Kachkachi, M. Nogués, E. Tronc, and D. Garanin, *J. Magn. Magn. Mater.* **221**, 158 (2000).
- [18] M. Bonfante, B. Hennion, F. Moussa, and G. Pepy, *Solid State Commun.* **10**, 553 (1972).
- [19] D. P. Landau, *J. Magn. Magn. Mater.* **200**, 231 (1999).
- [20] D. Mukamel and S. Krinsky, *Phys. Rev. B* **13**, 5065 (1976).
- [21] W. Neubeck, C. Vettier, D. Mannix, N. Bernhoeft, A. Hiess, L. Ranno, and D. Givord, in *Institute Laue Langevin Annual Reports*, 1998.
- [22] W. Neubeck, L. Ranno, M. Hunt, C. Vettier, and D. Givord, *Appl. Surf. Sci.* **138–139**, 195 (1999).
- [23] D. Bloch, D. Hermann-Ronzaud, C. Vettier, W. B. Yelon, and R. Alben, *Phys. Rev. Lett.* **35**, 963 (1975).
- [24] G. Cabrera, *Int. J. Mod. Phys. B* **4**, 1671 (1990).
- [25] K. Uzelac, A. Hasmy, and R. Jullien, *Phys. Rev. Lett.* **74**, 422 (1995).
- [26] S. Sako, Y. Umemura, K. Ohshima, M. Sakai, and S. Bandow, *J. Phys. Soc. Jpn.* **65**, 280 (1996).
- [27] Ping Sheng, R. Cohen, and J. Schrieffer, *J. Phys. C* **14**, L565 (1981).